analytical chemistry

Article

pubs.acs.org/ac

Zeolitic Imidazolate Framework-Based Electrochemical Biosensor for in Vivo Electrochemical Measurements

Wenjie Ma, Qin Jiang, Ping Yu, Lifen Yang,* and Lanqun Mao*

Beijing National Laboratory for Molecular Sciences, Key Laboratory of Analytical Chemistry for Living Biosystems, Institute of Chemistry, Chinese Academy of Sciences (CAS), Beijing 100190, China

Supporting Information

ABSTRACT: This study demonstrates the first exploitation of zeolitic imidazolate frameworks (ZIFs) as the matrix for constructing integrated dehydrogenase-based electrochemical biosensors for in vivo measurement of neurochemicals, such as glucose. In this study, we find that ZIFs are able to serve as a matrix for coimmobilizing electrocatalysts (i.e., methylene green, MG) and dehydrogenases (i.e., glucose dehydrogenase, GDH) onto the electrode surface and an integrated electrochemical biosensor is readily formed. We synthesize a series of ZIFs, including ZIF-7, ZIF-8, ZIF-67, ZIF-68, and ZIF-70 with different pore sizes, surface areas, and functional groups. The adsorption capabilities toward MG and GDH of these ZIFs are systematically studied with UV−vis spectroscopy, confocal laser scanning microscopy, and Fourier transfer-infrared spectroscopy. Among all the ZIFs demonstrated here, ZIF-70 shows excellent adsorption capacities toward both MG and GDH and is thus employed as the matrix for our glucose biosensor. To construct the biosensor, we first drop-coat a MG/ZIF-70 composite onto a glassy carbon electrode and then coat GDH onto the MG/ZIF-70 composite. In a continuous-flow system, the as-prepared ZIF-based biosensor is very sensitive to glucose with a linear range of 0.1−2 mM. Moreover, the ZIF-based biosensor is more highly selective on glucose than on other endogenous electroactive species in the cerebral system. In the end, we demonstrate that our biosensor is capable of monitoring dialysate glucose collected from the brain of guinea pigs selectively and in a near real-time pattern.

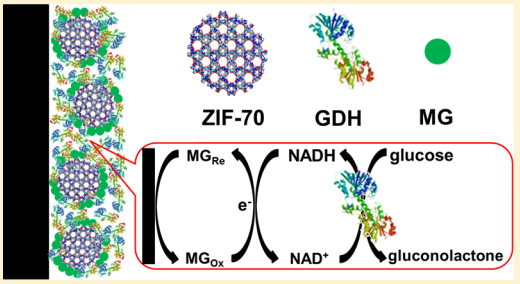

Ever increasing interests have been drawn in the development of analytical methods with excellent properties because the sustainable development in the environment, society, and economy essentially requires dramatic improvements for environmental monitoring, social safety guarantee, quality control, clinical diagnostics, and so forth.[1] Among the analytical methods demonstrated so far, electrochemical biosensors remain particularly attractive to meet such requirements because the integration of specific recognition of biorecognition elements (e.g., enzymes and aptamers) toward the targets with the technical simplicity and high sensitivity of electrochemical methods well endows the electrochemical biosensors with excellent properties, including good sensitivity, easy adaptability for rapid and on-spot analysis, and relatively cheap instrumentation.[2] One of the most challenging issues in this field is to develop a simple method to fabricate the biosensors reproducibly since surface confinement of multiple biosensing elements onto one electrode requires complicated and time-consuming processes for biosensor construction, which inevitably leads to unsatisfied reproducibility.[2] In this context, a matrix that is capable of simultaneously adsorbing multiple biosensing elements is highly desired to accomplish such a pursuit.[3] As a result, some kinds of porous materials such as silica, molecular sieve, and zeolites have been employed as a matrix for biosensor development.[4]

On the other hand, as one subclass of metal−organic frameworks (MOFs), zeolitic imidazolate frameworks (ZIFs) are an extensive class of hybrid solid-state materials self-assembled from metal ions or clusters with judiciously designed molecular building blocks into desired frameworks via coordination bonds.[5] This kind of coordination polymers has recently emerged as a novel type of crystalline porous materials combining the excellent properties of both zeolites and MOFs such as microporosity, high surface area, and exceptional thermal and chemical stability.[6] The framework of ZIFs contain regular pores and channels, allowing the entrance of guest molecules, and can differentiate species on a molecular level.[7] As a result of their fascinating structures and unique properties such as permanent nanoscale porosity, high surface areas and uniform-structured cavities,[8] ZIFs have been used for diverse applications, such as hydrogen storage,[9] gas separation,[10] catalysis,[11] and analytical applications, including sample collection and chromatographic separation.[12]

In addition to the promising applications mentioned above, the unique properties of ZIFs potentially result in a new paradigm for surface immobilization of biosensing elements, including biorecognition units and electrocatalysts for simple biosensor development because (i) the diverse porosity, pore sizes, and surface areas of ZIFs facilitate the adsorption of

Received: May 26, 2013
Accepted: July 1, 2013
Published: July 2, 2013

biosensing elements. (ii) The functional groups inherent in ZIFs interact with the biosensing elements, enhancing the adsorption capability of ZIFs. (iii) The high chemical stability of ZIFs endows a sustained framework integrity under various conditions, which essentially broadens the applications of the as-prepared biosensors. In spite of this great potentiality, to the best of our knowledge, the exploitation of ZIFs for electrochemical biosensor development has not been explored so far.

In this study, we demonstrate the first application of ZIF material as a matrix for developing electrochemical biosensors. We synthesize five typical ZIF materials {i.e., ZIF-7 [$Zn(bIm)_2$, HbIm = benzimidazole], ZIF-8 [$Zn(mIm)_2$, HmIm = 2-methylimidazole], ZIF-67 [$Co(mIm)_2$], ZIF-68 [Zn(bIm)-(nIm)], and ZIF-70 [$(Zn(Im)_{1.13}(nIm)_{0.87}$, HIm = imidazole, HnIm = 2-nitroimidazole]} with various structural topologies, functional groups, surface areas, metal centers, and pore sizes (Table S1 of the Supporting Information) and test their capability as a matrix for biosensor development, a glucose dehydrogenase-based biosensor to be exact. Among all the ZIFs demonstrated here, ZIF-70 is the best matrix for coimmobilization of MG and GDH. The as-prepared ZIF-based biosensor shows the excellent analytical properties such as selectivity and sensitivity for in vivo measurement of glucose. This study opens a simple yet effective approach to electrochemical biosensor development based on metal−organic framework science and technology.

EXPERIMENTAL SECTION

Reagents and Chemicals. Zinc nitrate hexahydrate [$Zn(NO_3)_2·6H_2O$], cobalt nitrate hexahydrate [$Co(NO_3)_2·6H_2O$], imidazole, benzimidazole, 2-methylimidazole, and 2-nitroimidazole were purchased from Aladdin Company and used without further purification. Glucose dehydrogenase (from *pseudomonas* species), *D*-(+)-glucose, and *β*-nicotinamide adenine dinuclotide (NAD^+) were all purchased from Sigma and used as supplied. Other chemicals were of at least analytical grade and used without further purification. Artificial cerebrospinal fluid (aCSF) used as a perfusion solution for in vivo microdialysis was prepared by mixing NaCl (126 mM), KCl (2.4 mM), KH_2PO_4 (0.5 mM), $MgCl_2$ (0.85 mM), $NaHCO_3$ (27.5 mM), Na_2SO_4 (0.5 mM), and $CaCl_2$ (1.1 mM) into Milli-Q water. Experiments were carried out with Milli-Q water from a Milli-pore system.

Syntheses of ZIFs. ZIF-7 nanocrystals were synthesized at room temperature, as described previously.[9a] Typically, a solution of $Zn(NO_3)_2·6H_2O$ (305.2 mg, 1.0 mmol) in 50 mL of DMF was rapidly poured into a solution of HbIm (770.2 mg, 6.5 mmol) in 50 mL of DMF under stirring. The mixture was stirred at room temperature for 48 h. Then, the product was centrifuged, washed with methanol three times, and dried at 100 °C. ZIF-8 nanocrystals were synthesized at room temperature, as described by Cravillo et al.[13] In a typical experiment, a solution of $Zn(NO_3)_2·6H_2O$ (293.2 mg, 1.0 mmol) in 20 mL of methanol was rapidly poured into a solution of HmIm (650.7 mg, 7.9 mmol) in 20 mL of methanol under stirring for 1 h. The nanocrystals were separated by centrifugation, washed with fresh methanol three times, and then dried at 100 °C. ZIF-67, ZIF-68, and ZIF-70 nanocrystals were synthesized through solvothermal reactions, as described in the literature.[9,7b,8a] For the synthesis of ZIF-67, a solution of $Co(NO_3)_2·6H_2O$ (581.2 mg, 2.0 mmol) in 10 mL of DMF was added into a solution of HmIm (327.8 mg, 4.0 mmol) in 20 mL of DMF. After being mixed thoroughly, the mixture was transferred into a 50 mL Teflon-lined autoclave, which was heated at 100 °C for 96 h in a programmable oven. For the synthesis of ZIF-68, 10 mL of HmIm (112.1 mg, 1.4 mmol) and HbIm (117.6 mg, 1.0 mmol) in DMF was added into 5 mL of $Zn(NO_3)_2·6H_2O$ (293.5 mg, 1.0 mmol) in DMF. After being mixed completely, the mixture was transferred into a 20 mL Teflon-lined autoclave, which was heated at 100 °C for 96 h in a programmable oven. For the synthesis of ZIF-70, 25 mL of HnIm (226.0 mg, 2.0 mmol) and HbIm (205.1 mg, 1.7 mmol) in DMF was added into 10 mL of $Zn(NO_3)_2·6H_2O$ (593.0 mg, 2.0 mmol) in DMF. After being mixed completely, the mixture was transferred into a 50 mL Teflon-lined autoclave, which was heated at 100 °C for 96 h in a programmable oven. The synthesized ZIF-67, ZIF-68, and ZIF-70 nanocrystals were washed with DMF (5 mL × 3) and dried in air.

The synthesized ZIFs were characterized by powder X-ray diffraction (XRD) using a Rigaku D/max 2500 X-ray diffractometer with Cu Kα radiation (λ = 1.54 Å) at a scan rate of 5 degree/min and scanning electron microscopy (SEM, S-4800, Hitachi, Japan). The results were shown in Figures S1−S5 of the Supporting Information.

Adsorption Capacities of ZIFs toward MG and GDH. To investigate the adsorption capacity of ZIFs toward the MG electrocatalyst, 4.0 mg of each kind of synthesized ZIFs was respectively dispersed into 4.0 mL of an aqueous solution of MG (20 μM). The mixtures were agitated at room temperature for 5 h and centrifuged. The resulting supernatants were collected for UV−vis spectroscopic measurements (TU-1900 spectrometer, Beijing, China). The absorbance at 650 nm was measured, and the adsorption capacities of ZIFs toward MG were calculated through the difference in the absorbance at 650 nm recorded for original MG solution and the supernatants, according to Lambert−Beer law.

MG/ZIF-70 composite was prepared by mixing ZIF-70 (20 mg) into a MG solution (20 μM, 20 mL) and agitating the mixture for 5 h at room temperature. The resulting precipitate (MG/ZIF-70) was washed with water three times, dried, and collected for the following investigation. For confocal laser scanning microscopy (CLSM) experiments, the obtained MG/ZIF-70 composite was dispersed in water and then the dispersion was coated onto glass. CLSM images were recorded by an Olympus FV1000-IX81 CLSM and a Leica TCS SP confocal system (Leica, Germany). The excitation (λ_{ex}) and emission (λ_{em}) wavelengths employed were 635 and 650 nm, respectively. Fourier transfer-infrared spectroscopy (FT-IR) spectra were conducted on a Bruker Tensor-27 FT-IR spectrometer (KBr pellet). The obtained MG/ZIF-70 composite was used for FT-IR measurements without further treatment. Similarly, ZIF-70 (0.5 mg) was dispersed into 50 μL of GDH solution (9.1 mg/mL), and the mixture was centrifuged to give a GDH/ZIF-70 composite. The composite was further air-dried for FT-IR measurements.

To calculate the adsorption capacities of GDH of ZIFs, 0.5 mg of ZIF-7, ZIF-8, ZIF-67, ZIF-68, and ZIF-70 was separately dispersed into 40 μL of aqueous solution of GDH (10 mg/mL). The resulting mixtures were agitated at room temperature for 30 min. The supernatants were collected and diluted 22.5 times for UV−vis spectroscopic measurements. The adsorption capacities of ZIFs toward GDH were calculated by converting the decrease in absorbance at 285 nm to the amount of GDH onto ZIFs, according to Lambert−Beer's law.

Electrochemical Measurements. Electrochemical measurements were performed with a computer-controlled electro-

dx.doi.org/10.1021/ac401576u | Anal. Chem. 2013, 85, 7550−7557

chemical analyzer (CHI 823B, Shanghai, China). Glassy carbon (GC, 3 mm diameter) electrodes for off-line electrochemical measurements were polished first with emery paper and then with aqueous slurries of fine alumina powder (0.3 and 0.05 μm) on a polishing cloth. The electrodes were finally rinsed with ethanol, acetone, and pure water under an ultrasonic bath at 5 min each. For electrode modification, a 10 mg MG/ZIF-70 composite was dispersed into 0.5 mL of water to give a homogeneous dispersion. Five microliters of the dispersion was drop coated onto GC electrodes to form MG/ZIF-70-modified electrodes. Off-line electrochemical experiments were carried out with the MG/ZIF-70-modified electrode as the working electrode, a platinum spiral wire as the auxiliary electrode, and a Ag/AgCl electrode (KCl saturated) as the reference electrode. A 0.10 M phosphate-buffered solution (pH 7.0) was used as the supporting electrolyte.

Online Monitoring of Glucose in Guinea Pig with ZIF-70-Based Biosensor. To demonstrate the application for in vivo neurochemical measurements, the ZIF-70-based biosensor was positioned into a thin-layer radial electrochemical flow cell for online monitoring of glucose in the microdialysates continuously sampled from the brains of guinea pigs. In this case, the ZIF-70-based biosensor was prepared by drop coating 10 μL of a MG/ZIF-70 dispersion (20 mg/mL) onto a GC electrode (6 mm diameter) first, and then drop coating 3 μL of GDH (10 mg/mL in phosphate-buffered solution, pH 7.0) onto the MG/ZIF-70-modified GC electrode. The electrode was then rinsed with water and air dried.

A ZIF-70-based online electrochemical detecting system was established by integrating a thin-layer radial electrochemical flow cell with a ZIF-70-based biosensor as the detector. The flow cell consists of a thin-layer radial flow block with a 50 μm gasket, in which ZIF-70-based biosensor was used as the working electrode, stainless steel as an auxiliary electrode, and the Ag/AgCl electrode (3.0 M NaCl) as the reference electrode.

In vivo microdialysis was performed under the procedures similar to those described in our previous work.[14] Briefly, adult male guinea pigs (300−400 g) were purchased from the Health Science Center, Peking University, and were housed on a 12:12 h light:dark schedule with food and water ad libitum. The animals were anaesthetized with chloral hydrate (345 mg/kg, i.p.) and put onto a stereotaxic frame. The microdialysis guide cannulas were implanted into the striatum using a standard stereotaxic procedure. The guide cannula was kept in place with three skull screws and dental cement. Stainless steel dummy blockers were inserted into the guide cannula and fixed until the insertion of the microdialysis probe. Throughout the surgery, the body temperature of the animals was maintained at 37 °C with a heating pad. Immediately after surgery, the guinea pigs were put into a warm incubator individually until they recovered from the anesthesia. The guinea pigs were allowed to recover for at least 24 h before in vivo microdialysis sampling. Prior to online electrochemical measurements, the microdialysis probes (CMA, dialysis length, 4.0 mm; diameter, 0.24 mm) were implanted into guinea pig striatum and were perfused with aCSF solution at 2.0 μL/min for at least 90 min for equilibration. Brain dialysate was continuously collected from guinea pig brain and mixed with NAD^+ (5.0 mM, 2.0 μL/min) perfused from another pump.

RESULTS AND DISCUSSION

Adsorption of Methylene Green with ZIFs. As a redox active dye, MG, has been frequently used as an electrocatalyst for electrochemical oxidation of β-nicotinamide adenine dinucleotide (reduced form, NADH), which is involved in the dehydrogenase-based bioelectrocatalytic and biosensing scheme. While ZIFs have been used for various applications such as gas storage and separation and catalysis, the utilization of ZIFs for the adsorption of MG electrocatalyst for biosensor development demonstrated in this study has not been reported to date. Figure 1 compares the UV−vis spectra recorded from

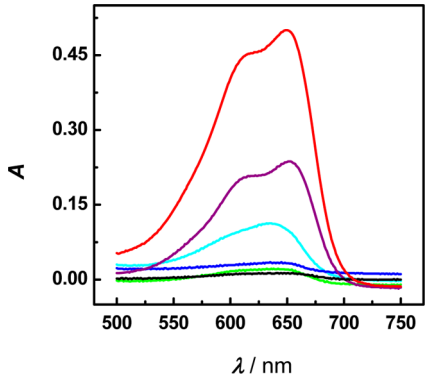

Figure 1. UV−vis spectra of MG solution (20 μM, red curve) and the supernatants of MG solutions with the addition of 4.0 mg of ZIF-68 (purple curve), ZIF-7 (cyan curve), ZIF-8 (blue curve), ZIF-67 (green curve), or ZIF-70 (black curve).

MG solution before (red curve) and after (curves with other colors) the addition of the same amount of each kind of synthesized ZIFs (i.e., ZIF-7, ZIF-8, ZIF-67, ZIF-68, and ZIF-70).

MG exhibits two absorption peaks at 610 and 650 nm, responsible for the $\pi \rightarrow \pi^*$ transition from the dimer and monomer of MG, respectively. The addition of each kind of ZIFs into solution clearly decreases the absorbance of both peaks. But the amplitude of the decrease varies remarkably according to the type of ZIFs. This result strongly suggests that MG adsorption activity depends on the ZIF type.

The adsorption capabilities of ZIF-7, ZIF-8, ZIF-67, ZIF-68, and ZIF-70 toward MG were evaluated with the decrease in the absorbance at 650 nm in the UV−vis spectra (Figure 1), and the results were summarized in Table 1. The adsorption capability of the ZIFs was in the order of ZIF-68 < ZIF-7 < ZIF-8 ≈ ZIF-67 < ZIF-70. ZIF-67 and ZIF-8 exhibit similar adsorption capacities mainly because they contain the same ligand and have almost the same d_a (3.4) and d_p (11.6) values and similar surface areas (1470 $m^2\ g^{-1}$ for ZIF-8 and 1319 $m^2\ g^{-1}$ for ZIF-67) (Table S1 of the Supporting Information). ZIF-7 and ZIF-68, both consisting of the benzimidazole ligand, show low adsorption capabilities presumably due to a large volume of the ligand and low surface areas and small d_p values as well. Among all ZIFs studied, ZIF-70 possesses the highest adsorption capacity toward MG (as high as 7.1 mg/g), which was attributed to its high surface area (1730 $m^2\ g^{-1}$) and large d_a (13.1) and d_p (15.9) values. The highest adsorption capability of ZIF-70 toward MG substantially enables its application as a matrix for biosensor development, as demonstrated later.

dx.doi.org/10.1021/ac401576u | Anal. Chem. 2013, 85, 7550−7557

Table 1. Structures of ZIFs and Their Adsorption Capacities Toward MG and GDH

ZIFs	Ligand Structure	Crystal Structure	Adsorption Capacities of MG (q_m)/(mg/g)	Adsorption Capacities of GDH (q_m)/(mg/g)
ZIF-7 $Zn(bIm)_2$	bIm 		5.65	-
ZIF-8 $Zn(mIm)_2$	mIm 		6.79	88.3
ZIF-67 $Co(mIm)_2$	mIm 		6.98	110.4
ZIF-68 $Zn(bIm)(nIm)$	nIm 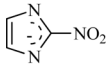 bIm 		3.82	584.9
ZIF-70 $Zn(Im)_{1.13}(nIm)_{0.87}$	Im  nIm 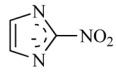		7.11	441.4

To clarify the adsorption site of MG on ZIF-70, on the surface, or within the pore, the obtained MG/ZIF-70 composite was scanned by a confocal laser scanning microscopy (CLSM) image, since this technique allows the study of the transport and distribution of dyes throughout crystals.[15] Figure 2 displays a three-dimensional CLSM image of the MG/ZIF-70

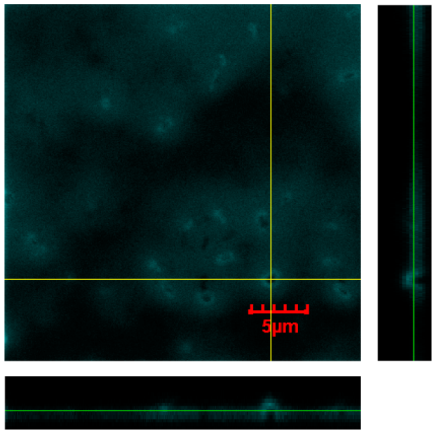

Figure 2. Three-dimensional confocal fluorescence image of MG/ZIF-70 composite (λ_{ex} = 635 nm, λ_{em} = 650 nm).

composite. MG is a weakly emissive dye, and the weak fluorescence observed from the surface of the MG/ZIF-70 composite suggests that MG was adsorbed on the surface of ZIF-70, possibly because of the relatively large molecular size of MG as compared to the pore size of ZIF-70.

We further investigated the adsorption of MG onto ZIF-70 by FT-IR. As displayed in Figure 3, free MG exhibits its ring

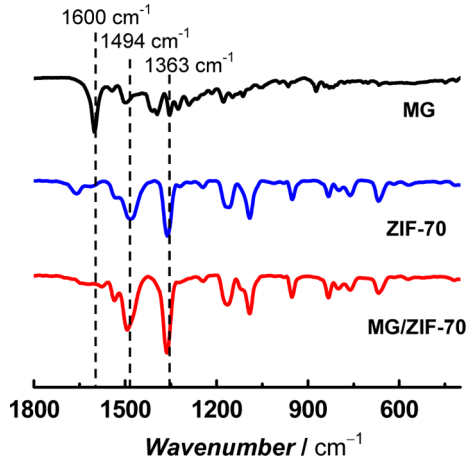

Figure 3. FT-IR spectra of MG, ZIF-70, and MG/ZIF-70. The *y* axis was presented in transmittance.

stretch at 1600 cm^{-1} (black curve). For ZIF-70 (blue curve), the peak at 1532 cm^{-1} was ascribed to the vibration of the C=C bond in the imidazole ring, and the peaks at 1362 and 1479 cm^{-1} were assigned to the symmetric and asymmetric stretching vibration of the $-NO_2$ group in nIm, respectively.[16] After MG adsorption (red curve), the ring stretch at 1600 cm^{-1} disappears and the peaks at 1362 and 1479 cm^{-1} shift to 1363, 1494 cm^{-1}, respectively, presumably suggesting that MG is adsorbed onto ZIF-70 through strong interactions such as

dx.doi.org/10.1021/ac401576u | *Anal. Chem.* 2013, 85, 7550−7557

hydrogen bonding and so on. This result demonstrates that the surface adsorption of MG on ZIF-70 is not merely a physical adsorption; chemical interactions between MG and ZIF-70 essentially result in the stable adsorption of the MG electrocatalyst onto ZIF-70.

In addition to the excellent adsorption capability of ZIF-70 toward the MG electrocatalyst, which facilitates the surface confinement of electrocatalysts for biosensor development, the as-confined MG electrocatalyst well maintains its electrochemical activity, as shown in Figure 4 A. To demonstrate such

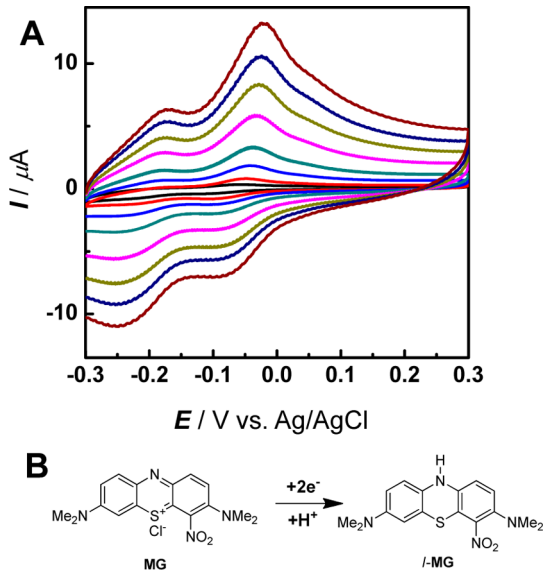

Figure 4. (A) CVs at the MG/ZIF-70-modified GC electrode in 0.10 M phosphate buffer (pH 7.0) at different scan rates of 10, 20, 50, 100, 200, 300, 400, and 500 mV s^{-1} (from inner to outer). (B) Illustration of the two-electron reduction of methylene green adsorbed onto ZIF-70 into leucomethylene green (*l*-MG).

a property, the MG/ZIF-70 composite was confined onto a GC substrate electrode and cyclic voltammetry was performed on the prepared MG/ZIF-70-modified electrode in phosphate buffer (pH 7.0). For comparison, cyclic voltammetry on a ZIF-70-modified GC electrode was also conducted. Within the electrochemical window employed, ZIF-70 shows no redox waves (data not shown), suggesting it is electrochemically inactive under the conditions employed here. While, on the other hand, the MG/ZIF-70 composite exhibits two pairs of redox waves at the formal potentials of −0.07 and −0.21 V, which were ascribed to the redox processes of the phenothiazine dye methylene green adsorbed onto ZIF-70 to leucomethylene green (*l*-MG),[17] as demonstrated in Figure 4 B. Furthermore, the linearity of the peak currents (at −0.07 V) against the potential scan rate (within a range from 10 to 500 mV s^{-1}) [I (μA) = 0.0136ν (mV/s) + 0.331, γ = 0.994] was good. And the peak potential was less dependent on the potential scan rate. These properties essentially suggest a fast and surface-confined electron transfer process of MG adsorption onto ZIF-70, which allows MG to well maintain its electrochemical activity after being adsorbed onto ZIF-70. We would also like to mention that the stable adsorption of MG onto ZIF-70 facilitates a stable CV peak current that remains almost unchanged upon continuously cycling the electrode for at least 50 times (data not shown). On the basis of these results, the MG/ZIF-70 composite substantially forms an excellent basis for the development of dehydrogenase-based electrochemical biosensors due to its fast electron transfer kinetics and stable adsorption, as will be demonstrated later.

Adsorption of GDH with ZIFs. As one of the most frequently used biorecognition units in glucose detection, GDH has good water solubility and is difficult to confine onto a conducting substrate. The common approach for GDH immobilization is based on a BSA-glutaraldehyde cross-linking method.[18] Figure 5 shows UV−vis spectra recorded for the

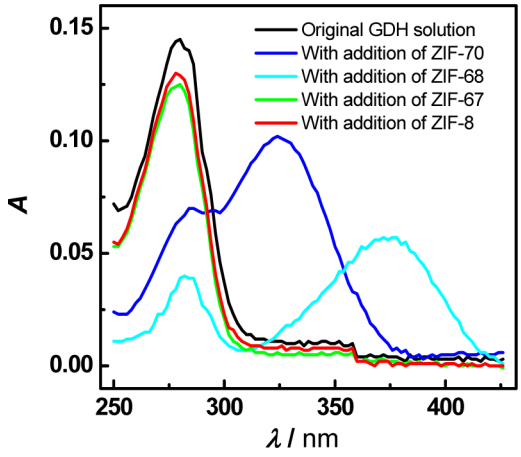

Figure 5. UV−vis absorption spectra of original GDH solution (black curve) and its supernatants obtained with the addition of 0.5 mg of ZIF-8 (red curve), ZIF-67 (green curve), ZIF-68 (cyan curve), or ZIF-70 (blue curve).

GDH solution before (black curve) and after (curves with other colors) the addition of the same amount of each kind of the synthesized ZIFs. GDH shows an absorption peak at around 285 nm, characteristic of the Soret band of GDH.[19] Decrease in the absorbance of this peak caused by the addition of each kind of ZIFs suggests that ZIFs can serve as a matrix for GDH adsorption and adsorption activities vary according to the kind of ZIFs. The adsorption capabilities of ZIFs toward GDH were estimated based on the difference between the amount of GDH in the initial solution and that in the supernatants. The amount of GDH was calculated from the decrease in absorbance of GDH at 285 nm according to Lambert−Beer's law. In the ZIFs tested here, ZIF-68 and ZIF-70 show strong absorbance bands around 366 and 336 nm, respectively, which partially overlay with that of GDH. To obtain the net absorbance for GDH in these cases, the absorbance of ZIF-68 or ZIF-70 at 285 nm was subtracted from the total absorbance of the supernatants at 285 nm. The amount of GDH adsorbed onto ZIFs was summarized in Table 1, in which the adsorption capabilities of different kinds of ZIFs toward GDH were in the order of ZIF-68 > ZIF-70 > ZIF-67 > ZIF-8. The difference in the adsorption capabilities of ZIFs toward GDH was understood in terms of different interactions between ZIFs and GDH and different surface areas of ZIFs. The interactions of protein/peptides with the solid surface are predominantly determined by the hydrophobic and electrostatic forces, which are two main types of driving forces in controlling the immobilization process and capacity of containing biomolecules into porous hosts.[20] The hydrophobicity of ZIFs makes them excellent adsorbents for immobilizing GDH through strong hydrophobic forces. For ZIF-68 and ZIF-70, they both have high surface areas and large pore sizes, resulting in their high adsorption capabilities for

dx.doi.org/10.1021/ac401576u | *Anal. Chem.* 2013, 85, 7550−7557

GDH. Moreover, ZIF-68 consists of stronger hydrophobic ligand benzimidazole than imidazole in ZIF-70 and thus exhibits stronger hydrophobic interaction with GDH and, as a result, higher adsorption capacity for GDH. As ZIF-70 shows a relatively high capability toward both MG and GDH, it was thus employed as a matrix for glucose biosensor construction.

In addition to hydrophobic interaction between GDH and ZIF-70 mentioned above, we have also studied other possible interactions such as donor−acceptor and H-bonding interactions between GDH and ZIF-70 by FT-IR, as displayed in Figure 6. For GDH, the band at 3285 cm^{-1} was attributed to the N−H stretching mode of the amidic binding of GDH. The bands at 2960 and 2936 cm^{-1} correspond to the C−H stretching of $-CH_2$ and $-CH_3$ groups.[4f,21] The bands at around 1656 and 1544 cm^{-1} were attributed to the amide I caused by C═O stretching vibrations of peptide linkages in the protein backbone and amide II resulted from a combination of N−H bending and C−N stretching, respectively.[21] FT-IR spectrum of ZIF-70 shows the absorption bands at 1362 and 1479 cm^{-1} from the vibration of N═O. Upon the adsorption of GDH on ZIF-70, the peak of C═O stretching vibration was clearly observed at 1656 cm^{-1} and the absorption peaks at 2936 cm^{-1} was assigned to the asymmetric stretching vibration of the $-CH_2$ group, suggesting that GDH was adsorbed onto ZIF-70. Furthermore, the absorption bands of the N═O vibration shift to 1489 and 1361 cm^{-1}, implying that the $-NH_2$ group in GDH interacts with ZIF-70 presumably through some interactions such as donor−acceptor and H-bonding interactions.[22] Similar to the interaction of MG with ZIF-70, these results also demonstrate that the adsorption of GDH on ZIF-70 may not be solely due to physical adsorption; however, the chemical interaction between GDH and ZIF-70 essentially enables the adsorption of the GDH biorecognition element onto ZIF-70. Note that, although MOFs have been used for immobilization of proteins, such as microperoxidase-11 and green fluorescent protein,[23] the uses of ZIFs as a matrix for the adsorption of GDH for biosensor development demonstrated here have not been reported so far.

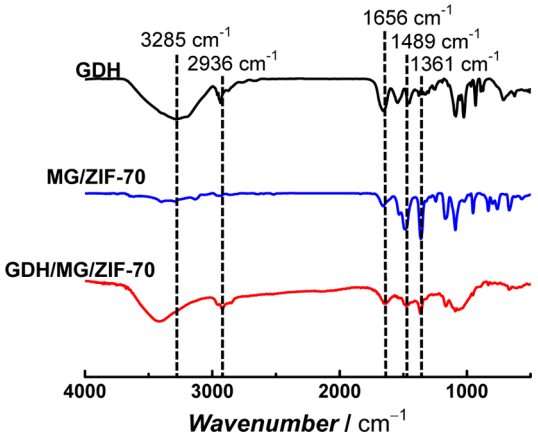

Figure 6. FT-IR spectra of GDH, ZIF-70, and GDH/ZIF-70. The *y* axis is presented in the transmittance.

Toward in Vivo Measurements. To demonstrate the application of ZIF-70-based biosensors for practical measurements, the as-prepared biosensors were used as the selective detector in a continuous-flow electrochemical cell, which was efficiently integrated with in vivo microdialysis to form a ZIF-70-based online electrochemical detecting system that could be used for near real-time monitoring of glucose change in the brain of living guinea pigs. In this case, aCSF was perfused from pump 1 (P1) into the brain of guinea pigs; the outflow dialysate was online mixed with an external solution containing NAD^+ perfused from pump 2 (P2) and finally measured in the electrochemical flow cell (Figure 7 A). Figure 7 B displays a typical amperometric response obtained with the ZIF-70-based

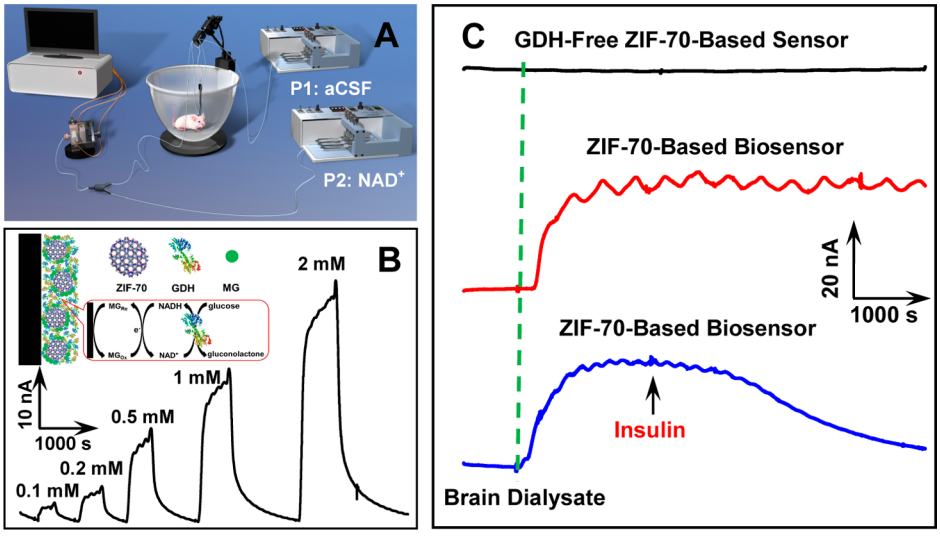

Figure 7. (A) Schematic illustration of the online electrochemical detecting system for in vivo monitoring of glucose in the cerebral system. (B) Online current−time response for glucose standards with concentrations indicated in the figure recorded on the online detecting system with a ZIF-70-based biosensor as the detector. Pure aCSF or aCSF containing standards was perfused into the system from pump 1 (P1) at 2 μL/min, and aCSF containing 5 mM NAD^+ was perfused from pump 2 (P2) at a rate of 2 μL/min. The biosensor was polarized at 0 V. Inset, schematic illustration of the ZIF-70-based biosensor. (C) Online current−time response recorded for the brain microdialysates of guinea pig on the online detecting systems with the MG/ZIF-70-modified GC electrode (i.e., GDH-free ZIF-70-based sensor, black line) and ZIF-70-based biosensor (red and blue line) as the detector. The brain microdialysate was continuously sampled from pump 1 (P1) and online mixed with pure NAD^+ solution (5.0 mM, aSCF) from pump 2 (P2). The perfusion rates for both pumps were 2 μL/min. The electrodes were polarized at 0 V.

dx.doi.org/10.1021/ac401576u | *Anal. Chem.* 2013, 85, 7550−7557

online electroanalytical system. Upon perfusion of the glucose solution containing NAD^+ at a perfusion rate of 2 μL/min, the currents obtained by this system have a linear range of 0.1−2 mM [I(nA) = 15.2 $C_{glucose}$ (mM) + 2.65, γ = 0.964], which well covers the physiological level of glucose,[1e,14b] substantially validating its application for continuously monitoring glucose in the cerebral system.

In addition to its good response to glucose, the ZIF-70-based online detecting system exhibits a high selectivity toward glucose. As documented in the previous studies,[14] a variety of electrochemically active species, such as sodium ascorbate (AA), 3,4-dihydroxyphenylacetic acid (DOPAC), dopamine (DA), uric acid (UA), and 5-hydroxytryptamine (5-HT), endogenously coexisting in rat brain could readily be oxidized on the online detector and may thus potentially interfere with the glucose measurement in brain microdialysates in this study. Thus, it is essential to test the selectivity of the ZIF-70-based system in vivo in the dialysate continuously sampled from the cortex of guinea pigs. For such a purpose, an online electrochemical detecting system was constructed with MG/ZIF-70 as the online detector (i.e., without GDH adsorption). As shown in Figure 7 C (black), upon microdialysate perfusion, no obvious current response was observed on such a system, demonstrating that the electroactive species such as AA, UA, DA, DOPAC, and 5-HT were not either oxidized or reduced on the MG/ZIF-70-based detector and thus did not interfere with the glucose sensing under the present conditions. Moreover, the ZIF-70-based system was quite stable for continuously sensing glucose in guinea pig brain. As displayed in Figure 7 C (red), the amperometric responses from brain glucose remained unchanged after continuously running the measurements for at least 100 min. With this system, we studied the change of the basal glucose following injection of insulin (2 units, in 200 μL normal saline) in vivo. As displayed in Figure 7 C (blue), upon the insulin injection, the current response recorded with our system decreased gradually, suggesting a decrease in the glucose level in guinea pig brain, which was consistent with the previous reports.[24] This study substantially validates the biosensor prepared with ZIFs, as a matrix for coadsorption of MG electrocatalyst and GDH for continuous measurements of glucose in the brain.

CONCLUSIONS

In summary, we, for the first time, demonstrate that ZIF materials can act as attractive matrices for immobilizing biosensing elements for the biosensor construction. The as-prepared ZIF-based biosensor shows a high selectivity and sensitivity toward glucose detection in the cerebral system, which is envisaged to be general for the development of new electrochemical biosensors with ZIFs as the matrices for coimmobilization of biosensing elements, including electrocatalysts and enzymes. This study demonstrates a first example that ZIFs can be used as one kind of unique matrix for the development of electrochemical biosensors with excellent analytical properties and promising applications.

ASSOCIATED CONTENT

Supporting Information

Additional information as noted in text. This material is available free of charge via the Internet at http://pubs.acs.org.

AUTHOR INFORMATION

Corresponding Author

*L.M.: e-mail, lqmao@iccas.ac.cn. L.Y.: e-mail, yanglf@iccas.ac.cn; fax, +86-10-62559373.

Notes

The authors declare no competing financial interest.

ACKNOWLEDGMENTS

The work was supported by the National Natural Science Foundation (Grants 21127901, 20935005, 21210007, 91213305 for L.M. and Grant 21175141 for L.Y.), the National Basic Research Program of China (Grants 973 program, 2010CB933502, 2013CB933704), and The Chinese Academy of Sciences (Grant KJCX2-YW-W25).

REFERENCES

(1) (a) Kimmel, D. W.; LeBlanc, G.; Meschievitz, M. E.; Cliffel, D. E. *Anal. Chem.* **2012**, *84*, 685−707. (b) Nichols, S. P.; Koh, A.; Storm, W. L.; Shin, J. H.; Schoenfisch, M. H. *Chem. Rev.* **2013**, *113*, 2528−2549. (c) Jung, J. H.; Cheon, D. S.; Liu, F.; Lee, K. B.; Seo, T. S. *Angew. Chem., Int. Ed.* **2010**, *49*, 5708−5711. (d) Kang, D.; Vallée-Bélisle, A.; Porchetta, A.; Plaxco, K. W.; Ricci, F. *Angew. Chem., Int. Ed.* **2012**, *51*, 6717−6721. (e) Jiang, Y.; Zhao, H.; Lin, Y.; Zhu, N.; Ma, Y.; Mao, L. *Angew. Chem., Int. Ed.* **2010**, *49*, 4800−4804.

(2) (a) Zhou, M.; Dong, S. *Acc. Chem. Res.* **2011**, *44*, 1232−1243. (b) Lu, X.; Cheng, H.; Huang, P.; Yang, L.; Yu, P.; Mao, L. *Anal. Chem.* **2013**, *85*, 4007−4013. (c) Huang, P.; Mao, J.; Yang, L.; Yu, P.; Mao, L. *Chem.—Eur. J.* **2011**, *17*, 11390−11393. (d) Heller, A.; Feldman, B. *Chem. Rev.* **2008**, *108*, 2482−2505. (e) Wang, J. *Chem. Rev.* **2008**, *108*, 814−825. (f) Ronkainen, N. J.; Halsall, H. B.; Heineman, W. R. *Chem. Soc. Rev.* **2010**, *39*, 1747−1763. (g) Yu, P.; Zhou, H.; Cheng, H.; Qian, Q.; Mao, L. *Anal. Chem.* **2011**, *83*, 5715−5720.

(3) Wang, J. *Analytical Electrochemistry*; Wiley-VCH: Hoboken, NJ, 2006.

(4) (a) Lazzara, T. D.; Mey, I.; Steinem, C.; Janshoff, A. *Anal. Chem.* **2011**, *83*, 5624−5630. (b) Liu, B.; Hu, R.; Deng, J. *Anal. Chem.* **1997**, *69*, 2343−2348. (c) Rahman, M. A.; Noh, H.-B.; Shim, Y.-B. *Anal. Chem.* **2008**, *80*, 8020−8027. (d) Vamvakaki, V.; Hatzimarinaki, M.; Chaniotakis, N. *Anal. Chem.* **2008**, *80*, 5970−5975. (e) Wang, B.; Li, B.; Deng, Q.; Dong, S. *Anal. Chem.* **1998**, *70*, 3170−3174. (f) Yang, S.; Jia, W.-Z.; Qian, Q.-Y.; Zhou, Y.-G.; Xia, X.-H. *Anal. Chem.* **2009**, *81*, 3478−3484. (g) Liu, S.; Chen, A. *Langmuir* **2005**, *21*, 8409−8413.

(5) Phan, A.; Doonan, C. J.; Uribe-Romo, F. J.; Knobler, C. B.; O'Keeffe, M.; Yaghi, O. M. *Acc. Chem. Res.* **2010**, *43*, 58−67.

(6) (a) Bétard, A.; Fischer, R. A. *Chem. Rev.* **2012**, *112*, 1055−1083. (b) Kreno, L. E.; Leong, K.; Farha, O. K.; Allendorf, M.; Van Duyne, R. P.; Hupp, J. T. *Chem. Rev.* **2012**, *112*, 1105−1125. (c) Li, J.-R.; Sculley, J.; Zhou, H.-C. *Chem. Rev.* **2012**, *112*, 869−932. (d) Stock, N.; Biswas, S. *Chem. Rev.* **2012**, *112*, 933−969. (e) Yang, L.; Kinoshita, S.; Yamada, T.; Kanda, S.; Kitagawa, H.; Tokunaga, M.; Ishimoto, T.; Ogura, T.; Nagumo, R.; Miyamoto, A.; Koyama, M. *Angew. Chem., Int. Ed.* **2010**, *49*, 5348−5351. (f) Mao, J.; Yang, L.; Yu, P.; Wei, X.; Mao, L. *Electrochem. Commun.* **2012**, *19*, 29−31.

(7) (a) Wang, B.; Côté, A. P.; Furukawa, H.; O'Keeffe, M.; Yaghi, O. M. *Nature* **2008**, *453*, 207−211. (b) Banerjee, R.; Phan, A.; Wang, B.; Knobler, C.; Furukawa, H.; O'Keeffe, M.; Yaghi, O. M. *Science* **2008**, *319*, 939−943. (c) Alkordi, M. H.; Liu, Y.; Larsen, R. W.; Eubank, J. F.; Eddaoudi, M. *J. Am. Chem. Soc.* **2008**, *130*, 12639−12641.

(8) (a) Banerjee, R.; Furukawa, H.; Britt, D.; Knobler, C.; O'Keeffe, M.; Yaghi, O. M. *J. Am. Chem. Soc.* **2009**, *131*, 3875−3877. (b) Park, K. S.; Ni, Z.; Côté, A. P.; Choi, J. Y.; Huang, R.; Uribe-Romo, F. J.; Chae, H. K.; O'Keeffe, M.; Yaghi, O. M. *Proc. Natl. Acad. Sci. U.S.A.* **2006**, *103*, 10186−10191.

(9) (a) Li, Y.-S.; Liang, F.-Y.; Bux, H.; Feldhoff, A.; Yang, W.-S.; Caro, J. *Angew. Chem., Int. Ed.* **2010**, *49*, 548−551. (b) Huang, A.;

Dou, W.; Caro, J. *J. Am. Chem. Soc.* **2010**, *132*, 15562−15564. (c) Wu, H.; Zhou, W.; Yildirim, T. *J. Am. Chem. Soc.* **2007**, *129*, 5314−5315.
(10) (a) Gücüyener, C.; van den Bergh, J.; Gascon, J.; Kapteijn, F. *J. Am. Chem. Soc.* **2010**, *132*, 17704−17706. (b) Li, K.; Olson, D. H.; Seidel, J.; Emge, T. J.; Gong, H.; Zeng, H.; Li, J. *J. Am. Chem. Soc.* **2009**, *131*, 10368−10369. (c) Venna, S. R.; Carreon, M. A. *J. Am. Chem. Soc.* **2010**, *132*, 76−78.
(11) (a) Wang, F.; Liu, Z.-S.; Yang, H.; Tan, Y.-X.; Zhang, J. *Angew. Chem., Int. Ed.* **2011**, *50*, 450−453. (b) Karagiaridi, O.; Lalonde, M. B.; Bury, W.; Sarjeant, A. A.; Farha, O. K.; Hupp, J. T. *J. Am. Chem. Soc.* **2012**, *134*, 18790−18796.
(12) (a) Bae, T.-H.; Lee, J. S.; Qiu, W.; Koros, W. J.; Jones, C. W.; Nair, S. *Angew. Chem., Int. Ed.* **2010**, *49*, 9863−9866. (b) Bux, H.; Liang, F.; Li, Y.; Cravillon, J.; Wiebcke, M.; Caro, J. *J. Am. Chem. Soc.* **2009**, *131*, 16000−16001. (c) Chang, N.; Gu, Z.-Y.; Yan, X.-P. *J. Am. Chem. Soc.* **2010**, *132*, 13645−13647. (d) Gu, Z.-Y.; Yang, C.-X.; Chang, N.; Yan, X.-P. *Acc. Chem. Res.* **2012**, *45*, 734−745.
(13) Cravillon, J.; Münzer, S.; Lohmeier, S.-J.; Feldhoff, A.; Huber, K.; Wiebcke, M. *Chem. Mater.* **2009**, *21*, 1410−1412.
(14) (a) Zhang, M.; Yu, P.; Mao, L. *Acc. Chem. Res.* **2012**, *45*, 533−543. (b) Lin, Y.; Liu, K.; Yu, P.; Xiang, L.; Li, X.; Mao, L. *Anal. Chem.* **2007**, *79*, 9577−9583. (c) Zhang, Z.; Zhao, L.; Lin, Y.; Yu, P.; Mao, L. *Anal. Chem.* **2010**, *82*, 9885−9891. (d) Zhuang, X.; Wang, D.; Lin, Y.; Yang, L.; Yu, P.; Jiang, W.; Mao, L. *Anal. Chem.* **2012**, *84*, 1900−1906. (e) Lin, Y.; Zhang, Z.; Zhao, L.; Wang, X.; Yu, P.; Su, L.; Mao, L. *Biosen. Bioelectron.* **2010**, *25*, 1350−1355. (f) Liu, K.; Lin, Y.; Yu, P.; Mao, L. *Brain Res.* **2009**, *1253*, 161−168.
(15) Han, S.; Wei, Y.; Valente, C.; Lagzi, I.; Gassensmith, J. J.; Coskun, A.; Stoddart, J. F.; Grzybowski, B. A. *J. Am. Chem. Soc.* **2010**, *132*, 16358−16361.
(16) (a) Cavalleri, B.; Ballotta, R.; Arioli, V.; Lancini, G. *J. Med. Chem.* **1973**, *16*, 557−560. (b) Cavalleri, B.; Volpe, G.; Arioli, V.; Pizzocheri, F.; Diena, A. *J. Med. Chem.* **1978**, *21*, 781−784.
(17) (a) Meredith, M. T.; Giroud, F.; Minteer, S. D. *Electrochim. Acta* **2012**, *72*, 207−214. (b) Wang, X.; Wang, J.; Cheng, H.; Yu, P.; Ye, J.; Mao, L. *Langmuir* **2011**, *27*, 11180−11186. (c) Akkermans, R. P.; Roberts, S. L.; Marken, F.; Coles, B. A.; Wilkins, S. J.; Cooper, J. A.; Woodhouse, K. E.; Compton, R. G. *J. Phys. Chem. B* **1999**, *103*, 9987−9995.
(18) Lei, C.; Deng, J. *Anal. Chem.* **1996**, *68*, 3344−3349.
(19) Nakamura, A.; Urabe, I.; Okada, H. *J. Bio. Chem.* **1986**, *261*, 16792−16794.
(20) (a) Hanefeld, U.; Gardossi, L.; Magner, E. *Chem. Soc. Rev.* **2009**, *38*, 453−468. (b) Mahmoudi, M.; Lynch, I.; Ejtehadi, M. R.; Monopoli, M. P.; Bombelli, F. B.; Laurent, S. *Chem. Rev.* **2011**, *111*, 5610−5637.
(21) (a) Chen, D.; Wang, Q.; Jin, J.; Wu, P.; Wang, H.; Yu, S.; Zhang, H.; Cai, C. *Anal. Chem.* **2010**, *82*, 2448−2455. (b) Wei, X.; Cruz, J.; Gorski, W. *Anal. Chem.* **2002**, *74*, 5039−5046. (c) Zhang, M.; Smith, A.; Gorski, W. *Anal. Chem.* **2004**, *76*, 5045−5050.
(22) (a) Panunto, T. W.; Urbanczyk-Lipkowska, Z.; Johnson, R.; Etter, M. C. *J. Am. Chem. Soc.* **1987**, *109*, 7786−7797. (b) Mrozek, R.; Głowiak, T. *J. Chem. Crystallogr.* **2004**, *34*, 153−157. (c) Janczak, J.; Perpétuo, G. J. *J. Mol. Struct.* **2010**, *975*, 166−172.
(23) (a) Lykourinou, V.; Chen, Y.; Wang, X.-S.; Meng, L.; Hoang, T.; Ming, L.-J.; Musselman, R. L.; Ma, S. *J. Am. Chem. Soc.* **2011**, *133*, 10382−10385. (b) Deng, H.; Grunder, S.; Cordova, K. E.; Valente, C.; Furukawa, H.; Hmadeh, M.; Gándara, F.; Whalley, A. C.; Liu, Z.; Asahina, S.; Kazumori, H.; O'Keeffe, M.; Terasaki, O.; Stoddart, J. F.; Yaghi, O. M. *Science* **2012**, *336*, 1018−1023.
(24) Vasylieva, N.; Barnych, B.; Meiller, A.; Maucler, C.; Pollegioni, L.; Lin, J.-S.; Barbier, D.; Marinesco, S. *Biosens. Bioelectron.* **2011**, *26*, 3993−4000.